Geochemical evidence for high-resolution variations during deposition of the Holocene S1 sapropel on the Cretan Ridge, Eastern Mediterranean

G. Gennari [a,*], F. Tamburini [b], D. Ariztegui [c], I. Hajdas [d], S. Spezzaferri [a]

[a] University of Fribourg, Department of Geosciences, Earth Sciences, Ch. du Musée 6, 1700 Fribourg, Switzerland
[b] Institute of Plant Nutrition, ETH Zurich, Eschikon 33, 8315 Lindau, Switzerland
[c] University of Geneva, Section of Earth Sciences, Rue des Maraîchers 13, 1205 Geneva, Switzerland
[d] Ion Beam Physics, PSI and ETH Zurich, Schafmattstrasse 20, 8093 Zurich, Switzerland

Major and minor element distributions and solid phase phosphorus contents were measured in a sediment core from the Cretan Ridge that contains the Holocene S1 sapropel. Micro-XRF ultra-high resolution analysis reveals multiple Mn peaks in the oxidized upper portion of the sapropel, which implies either a non-steady-state upward remobilization of Mn or not constant downward diffusion of bottom water oxygen. Sequential extraction allowed the identification of different phosphorus phases. Detrital phosphorus increases in the sapropel layer, suggesting enhanced delivery from land during sapropel deposition. Higher organic carbon to organic phosphorus ratios in the sapropel indicate enhanced regeneration of phosphorus relative to carbon under low-oxygen conditions. Fourier analysis on the ultra-high resolution XRF data reveals frequencies that are provisionally assigned to millennial to decennial solar cycles. Although these cycles have been reported from several continental and marine archives, they have never been documented from Sapropel S1 in the Eastern Mediterranean.

Keywords:
Sapropel
Chemical elements
Phosphorus
Cycles

1. Introduction

The Eastern Mediterranean Sea is characterized by the occurrence of organic matter-rich layers, termed sapropels. According to the original definition by Kidd et al. (1978), sapropels are well-delimited layers within open marine sediments, with thickness >1 cm and organic carbon content >2%. The relatively high organic carbon content of a sapropel is due to the combination of enhanced supply and limited degradation of organic matter at the sediment–water boundary, which is water-depth dependent (Murat and Got, 2000). Thereby, the difference between the organic carbon content of a sapropel and that of the surrounding sediments seems to be a more suitable parameter to define these layers (Murat, 1991; Ariztegui et al., 2000).

Among the various processes that have been invoked to explain sapropel formation (see Rohling, 1994 for a review), the "stagnation/anoxia" and the "increased productivity" models are the most discussed. According to the stagnation/anoxia model, anoxic bottom conditions are caused by a strong stratification of the water column that prevents vertical mixing and oxygen supply to the bottom waters. Different explanations have been proposed for the origin of this stratification: 1) Eurasian ice-sheet melt water entering the Mediterranean Sea (Olausson, 1961; Ryan, 1972; Aksu et al., 1995); 2) increased Nile river runoff linked to the periodic enhancement of the African–Asian monsoons (Rossignol-Strick 1983, 1985); 3) increased rainfalls and river discharge along the northern part of the Eastern Mediterranean Sea (Cramp et al., 1988; Rohling and Hilgen, 1991).

In the "increased productivity" model, sapropel deposition is linked to enhanced organic matter flux (Calvert, 1983; Calvert et al., 1992), since the present production of organic matter in the eastern Mediterranean cannot account for the high values of organic carbon (TOC) characterizing these layers (Calvert, 1983).

According to other authors (Castradori, 1993; Rohling, 1994; Emeis et al., 1998; Emeis et al., 2000), an increase of nutrient input via river runoff could have caused enhanced primary production and also promoted the stratification of the water column, coupling the two models. A significant increase of productivity at times of sapropel deposition is also revealed by paleo-productivity proxies, as Ba and marine barite concentration (e.g., Thomson et al., 1995, 1999; Martinez-Ruiz et al., 2000, 2003; Gallego-Torres et al., 2007). Enhanced productivity has also been explained with a radical change in the Mediterranean Sea circulation, from the modern anti-estuarine to an estuarine circulation (Sarmiento et al., 1988; Howell and Thunell, 1992). Results of recent modeling studies on thermohaline circulation suggest that a weakening of the present-day anti-estuarine circulation can lead to the deposition of enough organic carbon to account, at least, for the formation of the youngest sapropel S1 (Myers et al., 2000; Stratford et al., 2000). Uncertainties still exist regarding the

* Corresponding author. Fax: +41 26 300 97 42.
E-mail address: giordana.gennari@unifr.ch (G. Gennari).

extension of the anoxic/dysoxic layer in the water column; this layer has been described as a large water mass extending below the mixed layer (Murat and Got, 2000; Stratford et al., 2000), as well as an "anoxic blanket" above the sediment/water interface (Casford et al., 2003). More recently, Bianchi et al. (2006) suggest that a modified thermohaline circulation supplying oxygen only to the first 500 m of the water column may be responsible for the development of an anoxic blanket at the sea-floor, when coupled with higher productivity in the euphotic zone.

Regardless of the mechanism that led to their formation, sapropel occurrence is cyclic and is thought to be linked to minima in the precession cycle, corresponding to Northern Hemisphere summer insolation maxima, with a periodicity of about 21 kyr (Rossignol-Strick, 1983, 1985; Hilgen, 1991; Lourens et al., 1996).

In this research, we present a high-resolution geochemical study of sapropel S1, since any change in environmental or climatic conditions is reflected in major and minor element abundances (*e.g.*, Wehausen and Brumsack, 1998). Furthermore, because our proxy data offer a very detailed and continuous record, the identification of high-order cyclicities is attempted.

2. Materials and methods

Gravity core SIN97-01GC was collected on the morphological high between Crete and the Peloponnesus (35°49′07″ N, 22°42′02″ E; water depth 933 m) during the 15/97 cruise of R/V *Urania* (Fig. 1). Sampling for this study was limited to the uppermost part of the core (section 1; 0.0–68.0 cm bsf), since it contains a thick sapropel S1 overlaid by a few centimeters-thick oxidized interval, both interbedded in a hemipelagic muddy succession.

Sediment samples of 0.5 cm thickness for geochemical analyses were taken along the core at 3 cm spacing; a contiguous sampling was also performed at any change in sediment type or color. Sediments were then dried at room temperature and split into sub-samples. An aliquot of the material was gently ground in an agate mortar and passed through a sediment sieve (<125 μm), with the minimal extent of grinding necessary to achieve this size.

Table 1
Results of AMS ^{14}C dating on planktonic foraminifers. Calibration using OxCal 3.10 (Bronk Ramsey, 2005)

Lab code	Depth (cm)	Material	^{14}C age (yr BP)	Calibrated age (yr BP)
ETH-34228	1.0–2.0	Mixed planktonic foram	1050±55	610±70
ETH-34229	22.0–22.5	*Globigerinoides ruber*	6165±80	6570±180
ETH-34230	44.5–45.5	*Globigerinoides ruber*	11910±110	13405±235
ETH-34231	67.5–68.0	*Globigerinoides ruber*	17200±160	19925±375

A reservoir effect of 400 years was subtracted.

2.1. Organic matter

Organic matter characterization was performed at the University of Neuchâtel on about 80 mg of ground and sieved sediment with a Rock-Eval 6, using the standard whole rock pyrolysis method (Espitalié et al., 1986).

2.2. Phosphorus

Phosphorus was extracted from the dried sediment after grinding to <125 μm. A 5-step sequential extraction technique was used to distinguish among different phosphorus sedimentary phases (SEDEX method; Ruttenberg, 1992; Tamburini et al., 2002). Solid phases were progressively dissolved by using a series of extractants, each chosen in order to extract phosphorus associated with well defined sedimentary components: (1) loosely-bound P adsorbed on mineral surfaces, (2) iron and manganese oxy-hydroxides (referred in the text as CDB-P), (3) authigenic apatite, (4) detrital material (igneous, metamorphic and "aged" authigenic apatite), and (5) organic matter. The obtained sample solutions were diluted in milli-Q water and a color developing agent was added to the solutions following the ascorbic acid method for phosphate (Eaton et al., 1995). All the concentrations were then measured using a Perkin Elmer UV/Vis Spectrophotometer Lambda 10 at the GEA lab (University of Neuchâtel).

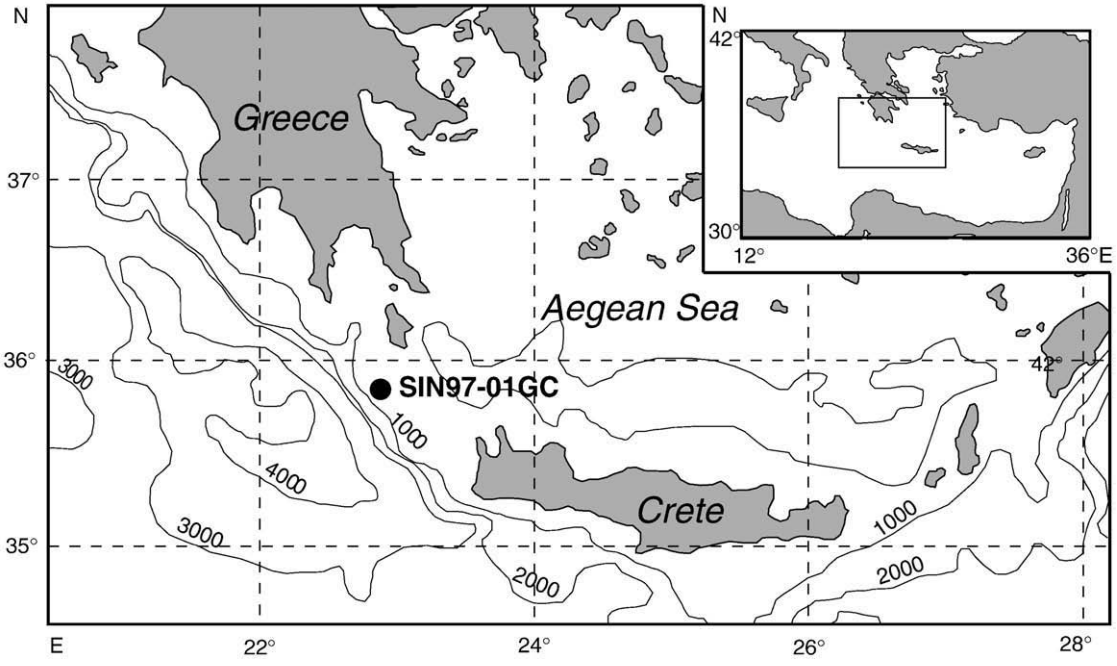

Fig. 1. Location map of core SIN97-01GC.

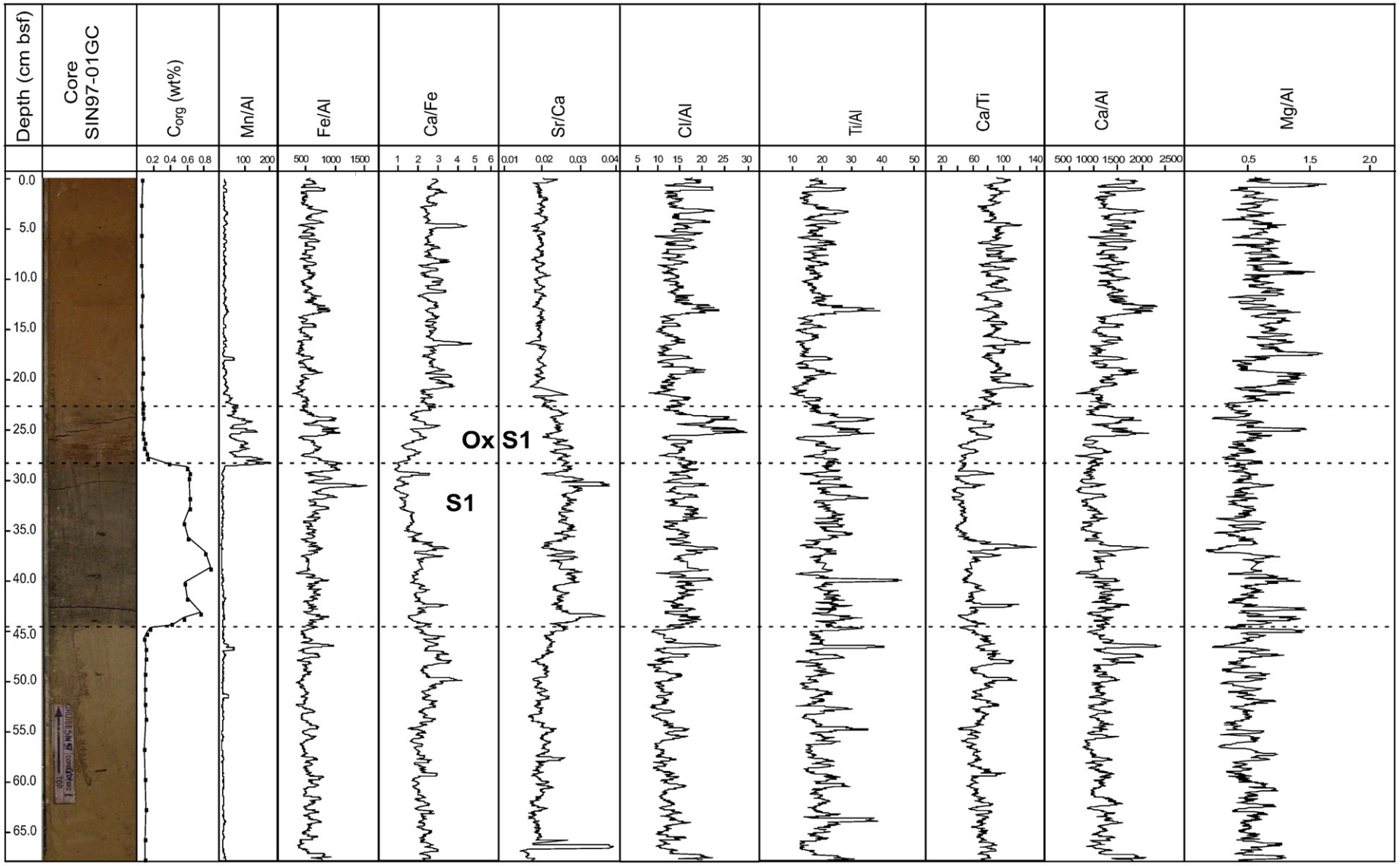

Fig. 2. C_{org} (weight %) and elemental ratios (versus Al, Fe or Ca). Elemental ratios were smoothed using a 10 points mobile average in order to highlight the dominant trends in the data. Ox S1:oxidized sapropel S1; S1: visual dark-colored sapropel S1.

Because of the reduction of Fe by dithionite and subsequent complexation by citrate, during the second step of this extraction it is possible to separate also ferric Fe (CDB-Fe). CDB-P and ferric Fe concentration were measured using a ICP-OES at the Soil Chemistry Institute of the ETH Zurich.

2.3. Elemental analyses

Ultra high-resolution qualitative analyses of major and minor elements (Mn, Fe, Ca, Mg, Al, Sr, Cl, Ti) were performed on macroscopic contiguous samples by X-ray microfluorescence (μ-XRF), using an EDAX Eagle III XPL μprobe (40 kV, 400 μA, 50/55 Dtm) with an analytical spot size of 50 μm. Average spacing between analytical points was 0.35 mm. Two profiles were acquired on two different sets of samples, giving consistent results. The μ-XRF elemental analyses were carried at the Section of Earth Sciences of the University of Geneva.

2.4. AMS ^{14}C dating

Radiocarbon ages were obtained using accelerator mass spectrometry (AMS) technique. The ^{14}C dating was performed at the AMS facilities, ETH and PSI in Zurich (Table 1). Four selected samples each containing 700 to 1000 specimens of planktonic foraminifers (15–18 mg of pure calcium carbonate) were hand-picked under a binocular microscope and then ultrasonically cleaned to remove any kind of contamination and/or diagenetic alteration. Samples were then dissolved in concentrated phosphoric acid (Hajdas et al., 2004a). The resulting carbon dioxide was then converted into graphite as described by Hajdas et al. (2004b). A reservoir age correction of 400 years (Siani et al., 2000) was applied to the obtained radiocarbon conventional ages, which were then calibrated using the program OxCal 3.10 (Bronk Ramsey, 2005).

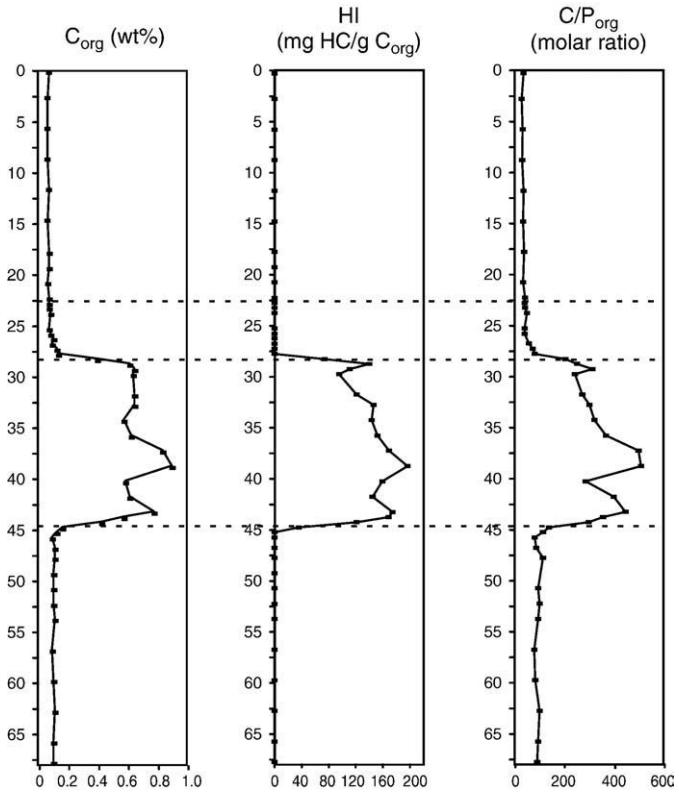

Fig. 3. C_{org} (wt%) concentration and HI (mg HC/g C_{org}), as determined by Rock-Eval, and C_{org}/P_{org} (molar ratio) curve.

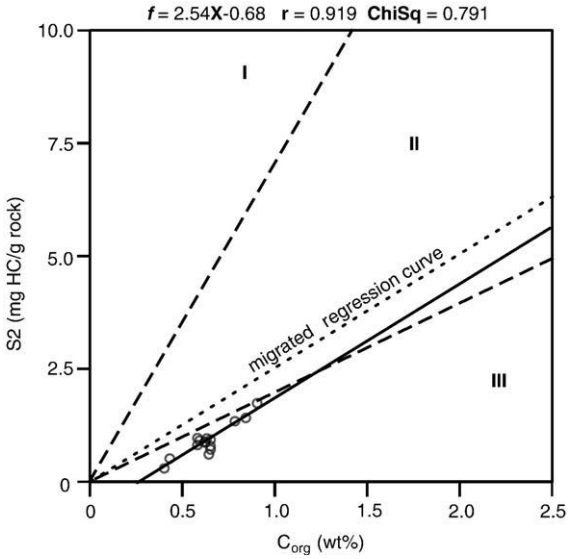

Fig. 4. S_2 versus C_{org} diagram for S1 samples. Boundaries between the three kerogen type fields (dashed lines) from Langford and Blanc-Valleron (1990). Regression curve (solid line) and migrated regression curve (dotted line) are also shown.

2.5. Fourier analysis

Four AMS ^{14}C ages (calibrated) were used to infer sedimentation rates and construct the chronological framework of the studied sedimentary sequence. To identify potential high-frequency cycles within the sedimentary record, Fourier analysis was performed on the obtained μ-XRF elemental ratio dataset (average of 33 points per cm). The Fourier analysis was carried out on selected elements versus Al ratios by using the software Analyseries (Paillard et al., 1996).

3. Results

3.1. Organic matter characterization by Rock-Eval

Organic carbon content in the studied core is generally low, but shows a remarkable increase in correspondence with the visual dark-colored sapropel (Fig. 2). Values range between 0.06 and 0.16 wt% in the "normal" hemipelagic sediments and from 0.39 to 0.89 wt% in sapropel S1.

T_{max} (420 °C on average) and hydrogen index (HI) values suggest that the organic material in sapropel S1 is mainly composed of partially degraded marine organic matter. Low HI values (75–200 mg HC/g C_{org}; Fig. 3) could indicate a strong mineral matrix effect (Espitalié et al., 1986). The S_2 versus C_{org} diagram (Fig. 4) confirms the presence of such matrix effect. In fact, according to Langford and Blanc-Valleron (1990), the regression line in a S_2 versus C_{org} diagram should pass through the axes origin, and a positive *x*-intercept, as in this case, could indicate the presence of rock-matrix effect. The high correlation degree of the samples in the S_2 versus C_{org} graph seems to indicate a common origin of the organic material. In fact, if the matrix effect is eliminated by migrating the regression line towards the axes origin, all the sapropel S1 samples fall in the marine organic matter field (type II kerogen field). Even though these results suggest that the main component of the organic material characterizing sapropel S1 is of marine origin, we do not exclude the contribution of terrestrial material. The amount of TOC in samples below and above the visual sapropel (<0.16 wt%) is too low, so it is not possible to distinguish the effect of clay mineral absorption.

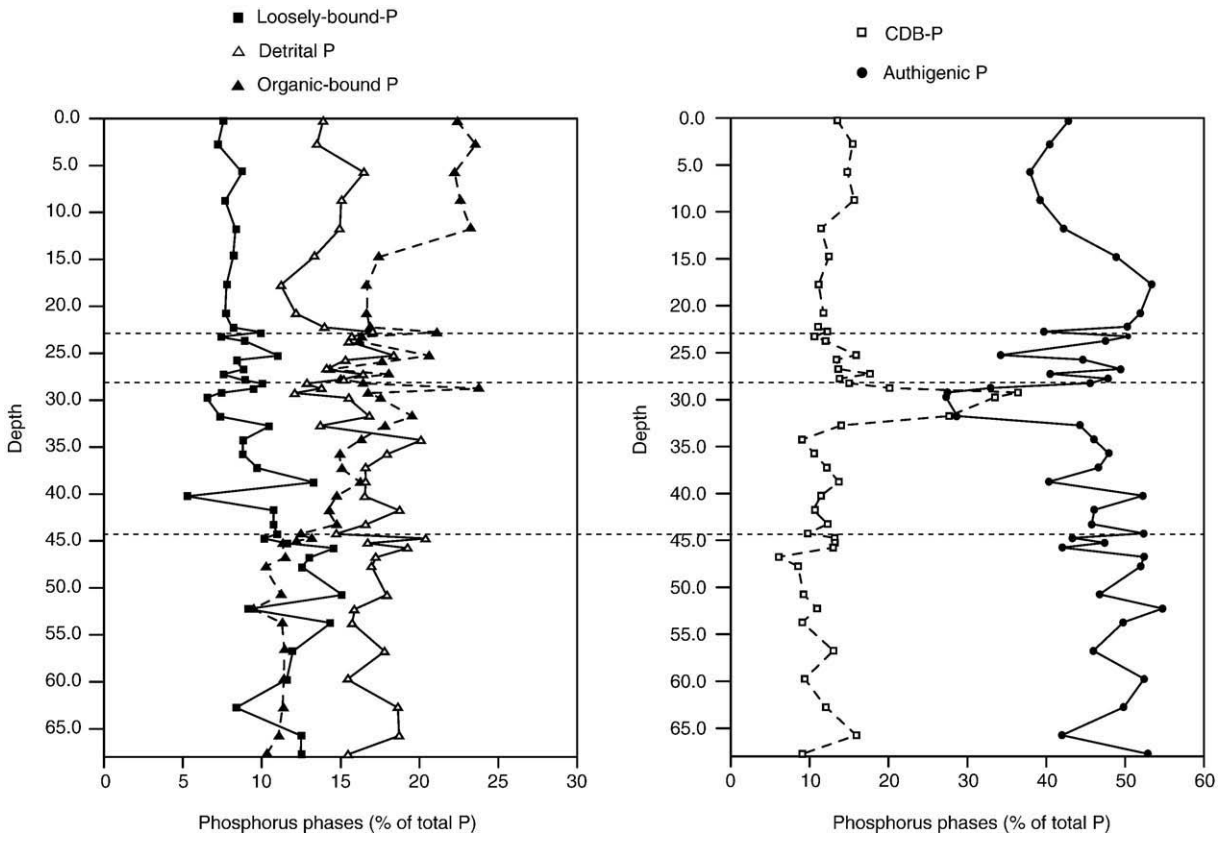

Fig. 5. Percentages of total P in the analyzed phosphorus sedimentary phases.

3.2. Phosphorus

Phosphorus extracted from sediments is dominated by the authigenic phase (apatite) that accounts on average for the 45% of total phosphorus (calculated as the sum of the extracted phases; Fig. 5). Both loosely-bound P and detrital P profiles (Fig. 6) show a general down-core increasing trend, while the organic-bound P is characterized by an opposite trend. Higher concentrations of detrital and, to a lesser extent, of organic-bound P are observed in the core interval between 28 and 44.5 cm bsf, corresponding to the visual sapropel. The sapropel S1 is also characterized, in the uppermost part, by a peak in CDB-P and in CDB-Fe. In this interval, CDB-P represents the most abundant solid phase (up to 37% of total P, Fig. 5).

The molar C_{org}/P_{org} (Fig. 3) is higher in the sapropel (200–500) in comparison to the overlying and underlying hemipelagic sediments (25–130). The sediments below S1, however, show C_{org}/P_{org} values slightly higher then the sediment above due to the general decreasing trend of organic-bound P.

3.3. Sediment geochemistry

The chemical characterization is presented as element/Al ratios (Fig. 2) in order to compensate for carbonate dilution (Wehausen and Brumsack, 1998). Fe, Mn and Al concentration curves are also shown for a comparison (Fig. 7). The Mn/Al ratio shows a remarkable increase at the top of the visual sapropel S1, developing a series of well-distinguished peaks in the oxidized part of the sapropel. The Fe/Al ratio shows a positive shift in the uppermost part of S1 and in the above 5 cm. Cl/Al and Ti/Al are both enriched in the core interval corresponding to the original sapropel (S1+Ox S1). Ca/Al and Mg/Al are covariant too, but with an opposite trend, and show depletion in the same interval. The Ca/Fe and Ca/Ti ratios decrease in the whole original sapropel interval, while Sr/Ca curve shows a positive shift in the same core interval.

3.4. ^{14}C chronology

Age assessment of core SIN97-01GC is based on four AMS ^{14}C ages obtained from planktonic foraminifers. The shallower sample (1–2 cm depth) was too small for monospecific dating, therefore mixed planktonic foraminifers were picked. Both radiocarbon conventional ages (referred in the text as ^{14}C yr) and calibrated ages (2σ error; referred as cal yr BP) are shown in Table 1.

The sediments immediately below the base of S1 sapropel are dated at 11910±110 ^{14}C yr BP (corresponding to 13405±235 cal yr BP), while the sample immediately above the top of the oxidized S1 displays an age of 6165±80 ^{14}C yr BP (corresponding to 6570±180 cal yr BP). Although there is general agreement in considering S1 to have been formed at around 9000–7000 years BP (see Fontugne et al., 1994 for a review), several authors reported older ages for the onset of the conditions leading to the formation of this anoxic layer (e.g., Troelstra et al., 1991; Howell and Thunell, 1992). In particular the age of the base of S1 in core SIN797-01GC is consistent with the ones reported by Rohling et al. (1993) for core T87/2/20G (11680 ^{14}C yr BP; 13300 cal yr BP reported in Hayes et al., 1999) and by Anastasakis (2007) for the south-eastern Mediterranean Sea.

The top of the visual sapropel has an inferred age of 7600 ^{14}C yr BP (corresponding to 8340 cal yr BP), well in agreement with the widely reported dating (Rohling, 1994; Mercone et al., 2000).

3.5. Fourier analysis

The sedimentation rate was calculated by fitting a regression line of calibrated ages against depth (Fig. 8). The calculated sedimentation rate is constant at 3.4 cm/kyr.

The performed spectral analysis shows well-distinguished periodicities with statistically significant peaks at 85–70, 60 and 50 years.

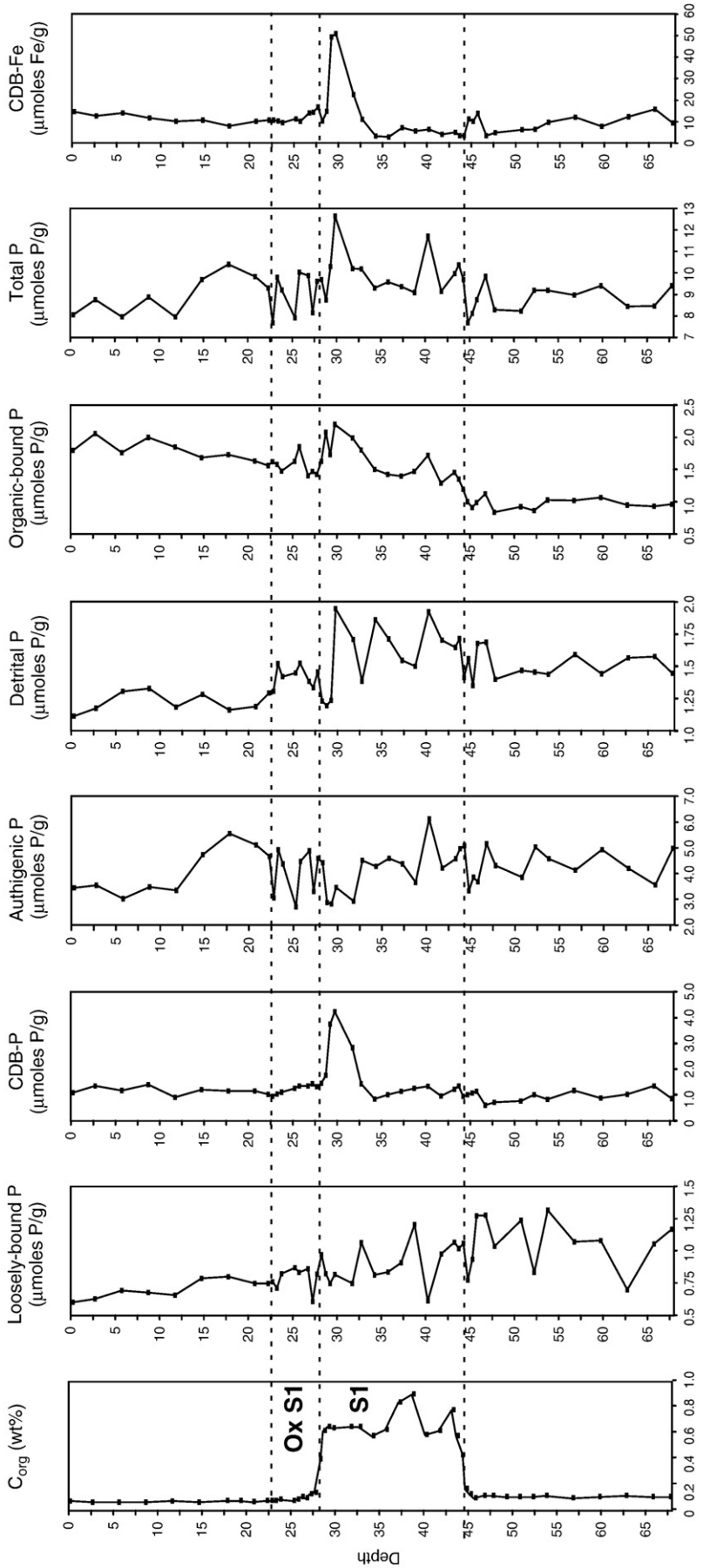

Fig. 6. Phosphorus solid phases content (in µmol P/g) and CDB-Fe (in µmol Fe/g). Ox S1:oxidized sapropel S1; S1: visual dark-colored sapropel S1.

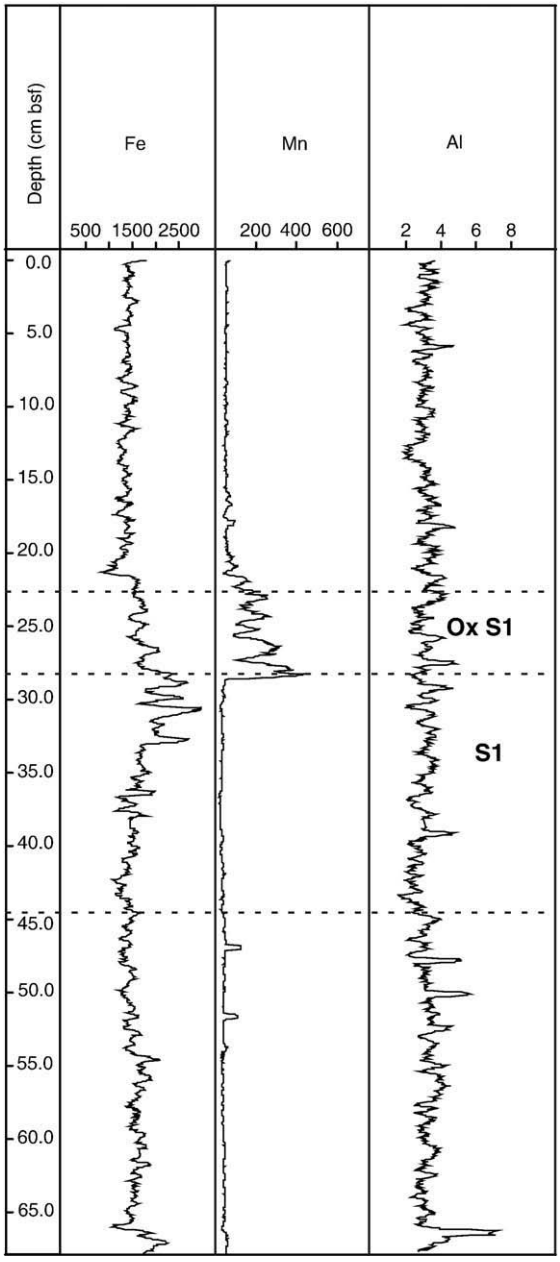

Fig. 7. Fe, Mn and Al concentrations (counts/second). All curves were smoothed using a 10 points mobile average in order to highlight the dominant trends in the data. Ox S1: oxidized sapropel S1; S1: visual dark-colored sapropel S1.

Millennial and centennial periodicities are also observed though not significant above the 95% confidence limit (see Fig. 9).

4. Discussion

4.1. TOC content and organic matter preservation

The visual dark dark-colored S1 sapropel from core SIN97-01GC is characterized by a TOC content distinctively higher than in the uppermost and lowermost sediments. The displayed values, ranging from 0.39 to 0.89 wt%, are however well below the 2% organic carbon content originally used to define these anoxic layers (Kidd et al., 1978). Indeed, lower TOC contents have been widely reported for sapropel S1 in the Eastern Mediterranean (e.g., Murat and Got, 2000). A linear relationship between TOC percentages and water depth, with values increasing with increasing location depth, has been clearly established by Murat and Got (2000). According with these authors, differences in organic carbon concentrations are more likely the result of variations in organic matter degradation than in organic matter availability, and are linked to lower degradation rates or to higher burial efficiency at deeper sites, resulting in increasing TOC content with depth. In this framework, the low TOC content of S1 on the Cretan Ridge fits well with the relatively shallow depositional environment (933 m).

As a consequence of the reduced preservation of organic matter, also the HI values are relatively low, as shown by the Rock-Eval results; this is in agreement with the positive linear correlation between HI and TOC concentration as also reported by Bouloubassi et al. (1999) for Pliocene–Pleistocene sapropels.

4.2. Phosphorus phases and C/P ratios

CDB-P and CDB-Fe show a peak at the top of S1, and not above the visual sapropel, as it was expected (Slomp et al., 2002, 2004). This is probably due to the presence of well-crystallized Fe oxides in the oxidized sapropel (Slomp et al., 1996) that are a less efficient sink for phosphorus in comparison with amorphous phases. The observed Fe enrichment can then be attributed to dissolution of amorphous Fe sulfides during the CDB step of the sequential extraction (Slomp et al., 1996). Both CDB-P and CDB-Fe curves, however, resemble closely the distribution shown by Slomp et al. (2002, 2004) suggesting that these peaks could anyway be related to the redox front.

Although the detrital P fraction extracted by the SEDEX method is operationally defined (Ruttenberg, 1992), and the extraction solution used (1 M HCl) might also dissolve sedimentary phases (e.g., clay and Fe minerals) that have resisted previous steps, we are confident that this fraction well represents detrital input. In fact, the amount of P contained in clays is negligible (Ruttenberg, 1992), and dithionite and citrate (step II) are the most efficient extractants for Fe oxides (Slomp et al., 1996). Generally, only well well-crystallized oxides might persist after this step, but these would probably also be of detrital origin.

Previous studies have shown that the detrital P well correlates with other detrital proxies, such as quartz and ice rafted debris (e.g. Tamburini et al., 2002, 2003) which were independently measured. Considering that, and knowing that detrital P is not involved in

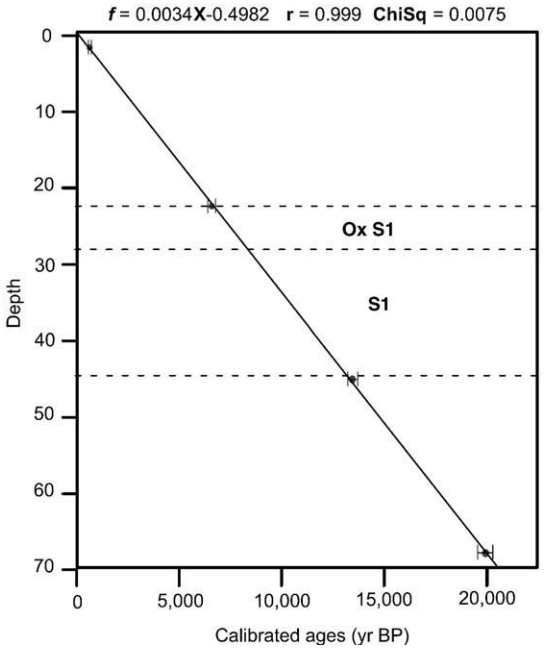

Fig. 8. Calibrated ^{14}C ages versus depth. Linear regression line is plotted.

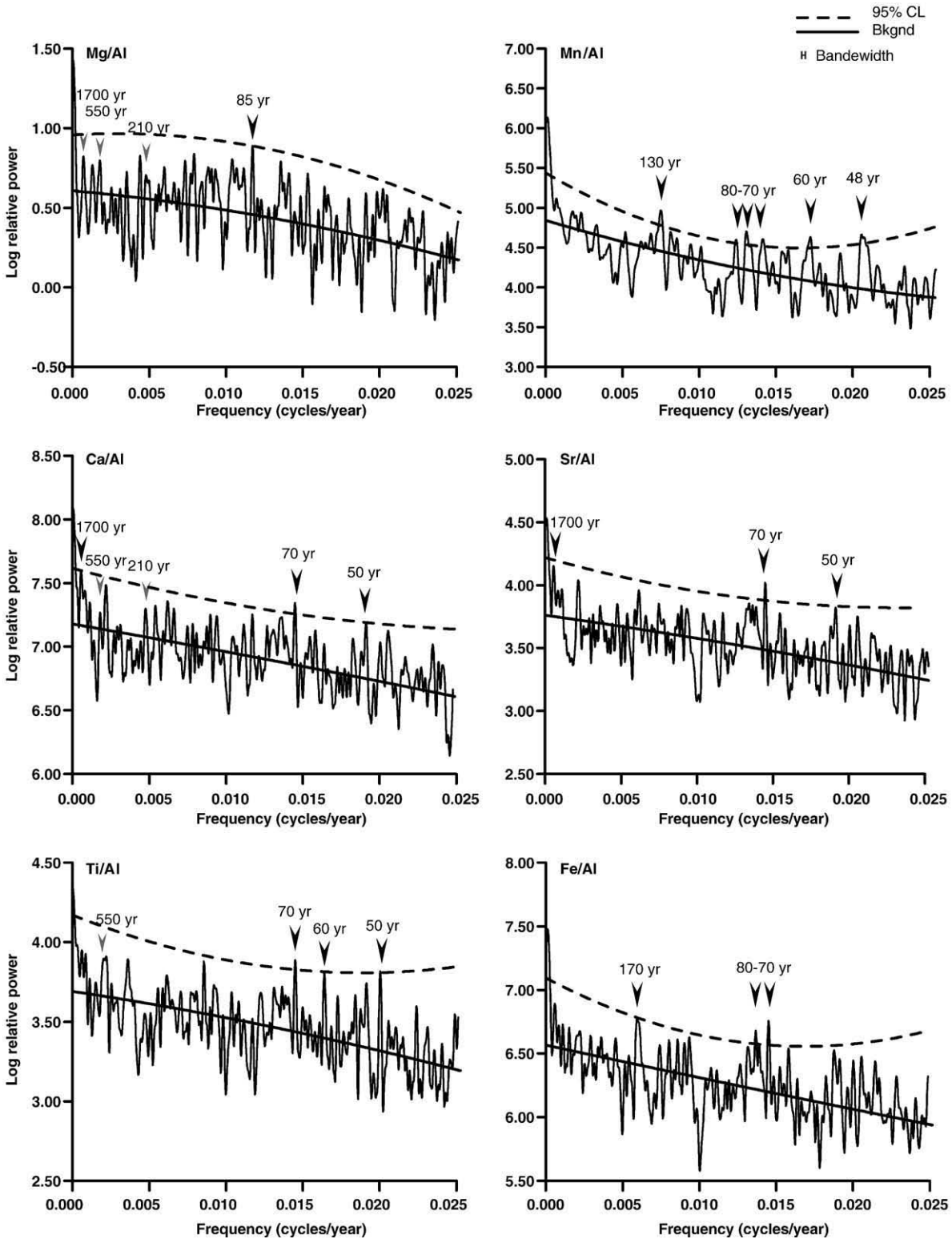

Fig. 9. Fourier analysis on Mg/Al, Mn/Al, Ca/Al, Sr/Al, Ti/Al and Fe/Al curves (B-Tuckey Spectrum, Bartlett window. Bandwidth: 0.0002522. Error estimation on Power spectrum: $0.546215 < \Delta P/P < 2.55813$). Sedimentation rates obtained by the regression curve of the calibrated ages versus depth plot.

biological P cycling, we consider its variations mainly as an indication of changes in detrital supply. In this case, its distribution indicates an increase of detrital input during sapropel S1 deposition, as also suggested by the slight increase of Ti/Al ratio in the core interval corresponding to the original sapropel.

Organic-bound P does not positively correlate with organic C. Because the organic matter in the sapropel is mainly of marine origin, as corroborated by our results and widely reported for the Eastern Mediterranean (e.g., Emeis et al., 1996), we can use a C/P Redfield ratio of 106–117 (Redfield et al., 1963; Anderson and Sarmiento, 1994) as a reference value for the original C/P ratio. In sapropel S1, C_{org}/P_{org} values are higher than the expected Redfield ratio, ranging from 200 to 500, while they display lower values in the overlying and underlying sediments (<130). Our data are consistent with an enhanced

regeneration of P in respect to C during sapropel deposition (Ingall and Jahnke, 1994; Slomp et al., 2002). The difference between the observed C_{org}/P_{org} values and the one reported by Slomp et al. (2002; C_{org}/P_{org}=300–1085 mol/mol) is consistent with the poor organic matter preservation evident in the low TOC and HI values.

4.3. Post-depositional alteration of sapropel S1

The geochemical signature of sapropel S1 from the Cretan Ridge is consistent with an active post-depositional oxidation due to the transition between different bottom water oxygenation levels at the end of the sapropel deposition (e.g., Thomson et al., 1999). Mn/Al peaks, and to a lesser extend the enrichment of Fe/Al observed in the oxidized sapropel, are linked to the downward penetration of the oxidation front (Van Santvoort et al., 1996), that led to post-depositional removal of organic matter, as evidenced in the uppermost part of the original sapropel. Nevertheless the Mn/Al profile shows a more articulated shape than the characteristic double peaks so far widely described (overview in Thomson et al., 1999). Van Santvoort et al. (1996) already illustrated the importance of sampling resolution in order to detect early diagenetic signals. As a case study, they showed the different shape of the solid phase Mn profile at low (1 peak; from 1 to >2.5 cm resolution) and high high-resolution (0.5 cm) sampling (2 peaks) (boxcore BC 12, Eastern Mediterranean). With a ultra-high resolution (0.3 mm), our Mn/Al curve shows multiple peaks that may derive from a non-constant upward flux of dissolved Fe^{2+} and Mn^{2+} and/or from a non-constant downward diffusion of bottom water oxygen, probably linked to rapid and short-lasting variations in sedimentation rates.

The Fe/Al curve presents a broad positive shift with respect to background values, because of increased amount of Fe-oxy-hydroxides (Ox S1) and of pyrite or other amorphous Fe-sulfates (from the top of the visual sapropel down to about 35 cm).

The Cl/Al profile may provide further evidence of the sapropel original thickness, being linked to the higher porosity that usually characterizes organic-rich sediments (Thomson et al., 1995).

The negative shift in Ca content with respect to both Fe and Sr can be related to differences in calcite preservation and abundance of Sr-rich aragonite, in S1 and in normal pelagic sediments.

4.4. High-frequency cyclicity

Millennial to decennial-scale periodicities have been observed at very different locations, in both marine and continental archives (e.g., Hulu cave, China; GISP2 and GRIP ice cores, Greenland; monsoon climate in Africa) and using different proxy records (see Tyson et al., 2002). Their origin is certainly related to solar activity (Bond et al., 2001), but the mechanisms of the complex interplay between sun and climate are still under debate (Beer et al., 2000; Bond et al., 2001; Turney et al., 2005).

Also in core SIN97-01GC, the Fourier analysis performed on the ultra-high resolution elemental ratio records reveals the presence of well-distinguished millennial to decennial cyclicities centered at around 1700, 550, 210, 85–70, 60 and 50 years (Fig. 9). The cycles detected in our records at 210 yr (Suess Cycles) and 85–70 yr (Gleissberg Cycles) are most likely related to solar variability (see Chambers et al., 1999 for a review). The 550 years periodicity has been detected in the Holocene GISP2 ice core (Greenland; Stuiver et al., 1995) and in North Atlantic sediment records (Chapman and Shackleton, 2000), giving indication of an interconnection between atmospheric and oceanic variability (Chapman and Shackleton, 2000). According to other authors (e.g., Debret et al., 2007) solar forcing could be a more probable explanation for these periodicities.

The 1700 years periodicity corresponds to the ~1800 yr frequencies already identified in lake sediment records, and it has been attributed to variation in insolation (Skilbeck et al., 2005).

Considering the known influence of changes in insolation in the Mediterranean and northern African region and their direct link to sapropel formation (e.g. Rossignol-Strick, 1985), the presence of these cycles confirms the strong sensitivity of Mediterranean climate even at a decennial scale.

5. Conclusions

Our high-resolution geochemical study of sapropel S1 from the Cretan Ridge (Eastern Mediterranean) shows that:

1) The top of the original sapropel was affected by post-depositional alteration by a downward penetrating oxidation front, resulting in the removal of organic matter. The ultra high-resolution μ-XRF elemental analysis reveals a more articulated Mn/Al profile than expected, with the development of a multiple peak pattern. This peculiar profile may be explained by a “not constant” upward migration of dissolved Fe and Mn and/or by a non-constant downward diffusion of bottom water oxygen, probably linked to rapid variations in the sedimentation rate.
2) The C_{org}/P_{org} ratio is in agreement with an enhanced regeneration of phosphorus in respect to C caused by low low-oxygen content of bottom waters and sediments (Ingall and Jahnke, 1994) during sapropel deposition (Slomp et al., 2002).
3) Though aware of a possible analytical bias, we consider detrital phosphorus as a reliable indicator of detrital supply from the continent. In this case, its increase supports the hypothesis of an enhanced detrital input during sapropel S1 deposition.
4) The very high-resolution proxy record obtained by XRF analysis allowed us to perform a spectral analysis. High-frequency millennial to decennial-scale solar cycles centered at 1700, 550, 210, 85–70, 60 and 50 years were identified, suggesting that also during sapropel S1 deposition, climate in the Mediterranean region was paced by solar variability even at short periodicities. Our approach suggests that the use of μ-XRF scanning technique is a powerful tool that can be used in order to obtain high high-resolution records suitable for the identification of meaningful periodicities.

Acknowledgements

We warmly thank Cesare Corselli and Daniela Basso for providing the core material, Thierry Adatte for the Rock-Eval analyses and Kurt Barmettler for ICP-OES measurements. We also thank Phil Meyers and two anonymous reviewers for their useful revision of the manuscript.

This research is funded by the Swiss National Foundation (Ref. 200021-111694).

References

Aksu, A.E., Yasar, D., Mudie, P.J., 1995. Paleoclimatic and paleoceanographic conditions leading to development of sapropel layer S1 in the Aegean Sea. Palaeogeogr. Palaeoclimatol. Palaeoecol. 116, 71–101.

Anastasakis, G., 2007. Clay mineral distribution patterns in the southeastern Mediterranean Sea during the late Quaternary. Geol. Carpath. 58 (4), 383–395.

Anderson, L.A., Sarmiento, J.L., 1994. Redfield ratios of remineralization determined by nutrients data analysis. Glob. Biogeochem. Cycles 8 (1), 65–80.

Ariztegui, D., Asioli, A., Lowe, J.J., Trincardi, F., Vigliotti, L., Tamburini, F., Chondrogianni, C., Accorsi, C.A., Bandini Mazzanti, M., Mercuri, A.M., van der Kaars, S., McKenzie, J.A., Oldfield, F., 2000. Palaeoclimatic reconstructions and formation of sapropel S1: inferences from Late Quaternary lacustrine and marine sequences in the Central Mediterranean region. Paleogeogr. Paleoclimatol. Palaeoecol. 158, 215–240.

Beer, J., Mende, W., Stellmacher, R., 2000. The role of the sun in climate forcing. Quat. Sci. Rev. 19, 403–415.

Bianchi, D., Zavatarelli, M., Pinardi, N., Capozzi, R., Capotondi, L., Corselli, C., Masina, S., 2006. Simulations of ecosystem response during the sapropel S1 deposition event. Paleogeogr. Paleoclimatol. Palaeoecol. 235, 265–287.

Bond, G., Kromer, B., Beer, J., Muscheler, R., Evans, M.N., Showers, W., Hoffman, S., Lotti-Bond, R., Hajdas, I., Bonani, G., 2001. Persistent solar influence on North Atlantic climate during the Holocene. Science 294, 2130–2136.

Bouloubassi, I., Rullkötter, J., Meyers, P.A., 1999. Origin and transformation of organic matter in Pliocene–Pleistocene Mediterranean sapropels: organic geochemical evidence reviewed. Mar. Geol. 153, 177–197.

Bronk Ramsey, C., 2005. Improving the resolution of radiocarbon dating by statistical analysis. In: Levy, T.E., Higham, T.F.G. (Eds.), The Bible and Radiocarbon Dating: Archaeology, Text and Science. Equinox, London, pp. 57–64.

Calvert, S.E., 1983. Geochemistry of the Pleistocene sapropels and associated sediments from the Eastern Mediterranean. Oceanol. Acta 6, 225–267.

Calvert, S.E., Nielsen, B., Fontugne, M.R., 1992. Evidence from nitrogen isotope ratios for enhanced productivity during formation of eastern Mediterranean sapropels. Nature 359, 223–225.

Casford, J.S.L., Rohling, E.J., Abu-Zied, R.H., Fontanier, C., Jorissen, F.J., Leng, M.J., Schmiedel, G., Thomson, J., 2003. A dynamic concept for eastern Mediterranean circulation and oxygenation during sapropel formation. Palaeogeogr. Palaeoclimatol. Palaeoecol. 190, 103–119.

Castradori, D., 1993. Calcareous nannofossils and the origin of eastern Mediterranean sapropels. Paleoceanography 8, 459–471.

Chambers, F.M., Ogle, M.I., Blackford, J.J., 1999. Palaeoenvironmental evidence for solar forcing of Holocene climate: linkages to solar science. Prog. Phys. Geogr. 23, 181–204.

Chapman, M.R., Shackleton, N.J., 2000. Evidence of 550-year and 1000-year cyclicities in North Atlantic circulation patterns during the Holocene. Holocene 10 (3), 287–291.

Cramp, A., Collins, M., West, R., 1988. Late Pleistocene–Holocene sedimentation in the NW Aegean Sea: a paleoclimatic–paleoceanographic reconstruction. Palaeogeogr. Palaeoclimatol. Palaeoecol. 68, 61–77.

Debret, M., Bout-Roumazeilles, V., Grousset, F., Desmet, M., McManus, J.F., Massei, N., Sebag, D., Petit, J.R., Copard, Y., Trenteseaux, A., 2007. The origin of the 1500-year climate cycles in Holocene North-Atlantic records. Clim. Past 3, 569–575.

Eaton, A.D., Clesceri, L.S., Greenberg, A.E., 1995. Standard Methods for the Examination of Water and Wastewater, 19th Ed. American Public Health Association, Washington, D.C.

Emeis, K.C., Robertson, A.H.F., Richter, C., et al., 1996. Proc. ODP. Init. Repts., 160. Ocean Drilling Program, College Station, TX.

Emeis, K.C., Schulz, H.M., Struck, U., Sakamoto, T., Doose, H., Erlenkeuser, H., Howell, M., Kroon, D., Paterne, M., 1998. Stable isotopes and temperature records of sapropels from ODP Sites 964 and 967: constraining the physical environment of sapropel formation in the Eastern Mediterranean Sea. In: Robertson, A.H.F., Emeis, K.-C., Richter, C., Camerlenghi, A. (Eds.), Proc. ODP, Sci. Results, 160. Ocean Drilling Program, College Station, TX, pp. 309–331.

Emeis, K.C., Struck, U., Schulz, H.M., Rosenberg, R., Bernasconi, S., Erlenkeuser, H., Sakamoto, T., Martinez-Ruiz, F., 2000. Temperature and salinity variations of Mediterranean Sea surface waters over the last 16.000 years from records of planktonic stable oxygen isotopes and alkenone unsaturation ratios. Palaeogeogr. Palaeoclimatol. Palaeoecol. 158, 259–280.

Espitalié, J., Deroo, G., Marquis, F., 1986. La pyolyse Rock-Eval et ses applications — III partie. Rev. Inst. Fr. Pet. 41 (1), 73–89.

Fontugne, M.R., Arnold, M., Labeyrie, L., Paterne, M., Calvert, S.E., Duplessy, J.C., 1994. Paleoenvironment, sapropel, chronology and Nile river discharge during the last 20,000 years as indicated by deep-sea sediment records in the eastern Mediterranean. In: Bar-Yosef, O., Kra, R.S. (Eds.), Late Quaternary Chronology and Paleoclimate of the eastern Mediterranean. Radiocarbon, pp. 75–88.

Gallego-Torres, D., Martinez-Ruiz, F., Paytan, A., Jiménez-Espejo, F.J., Ortega-Huertas, M., 2007. Pliocene–Holocene evolution of depositional conditions in the eastern Mediterranean: role of anoxia vs. productivity at time of sapropel deposition. Palaeogeogr. Palaeoclimatol. Palaeoecol. 246, 424–439.

Hajdas, I., Bonani, G., Zimmerman, S.H., Mendelson, M., Hemming, S., 2004a. C-14 ages of ostracodes from Pleistocene lake sediments of the western Great Basin, USA—Results of progressive acid leaching. Radiocarbon 46, 189–200.

Hajdas, I., Bonani, G., Thut, J., Leone, G., Pfenninger, R., Maden, C., 2004b. A report on sample preparation at the ETH/PSI AMS facility in Zurich. Nucl. Inst. Methods Sec. B 223–224, 267–271.

Hayes, A., Rohling, E.J., De Rijk, S., Kroon, D., Zachariasse, W.J., 1999. Mediterranean planktonic foraminiferal faunas during the last glacial cycle. Mar. Geol. 153, 239–252.

Hilgen, F.J., 1991. Extension of the astronomically calibrated (polarity) time scale to the Miocene/Pliocene boundary. Earth Planet Sci. Lett. 107, 349–368.

Howell, M.W., Thunell, R.C., 1992. Organic carbon accumulation in Bannock Basin: evaluating the role of the productivity in the formation of eastern Mediterranean sapropels. Mar. Geol. 103, 461–471.

Ingall, E., Jahnke, R., 1994. Evidence for enhanced phosphorus regeneration from marine sediments overlain by oxygen depleted waters. Geochim. Cosmochim. Acta 58 (11), 271–275.

Kidd, R.B., Cita, M.B., Ryan, W.B.F., 1978. Stratigraphy of eastern Mediterranean sapropel sequences recovered during DSDP Leg 42A and their paleoenvironmental significance. In: Hsü, K.J., Montadert, L., et al. (Eds.), init. Rep. DSDP, 423 (pt. 1). US Government Printing Office, Washington, DC, pp. 421–443.

Langford, F.F., Blanc-Valleron, M.M., 1990. Interpreting Rock-Eval pyrolysis data using graphs of pyrolizable hydrocarbons vs. total organic carbon. A.A.P.G. Bul. 74 (6), 799–804.

Lourens, L.J., Antonarakou, A., Hilgen, F.J., van Hoof, A.A.M., Vergnaud-Grazzini, C., Zachariasse, W.J., 1996. Evaluation of the Plio-Pleistocene astronomical time-scale. Paleoceanography 11, 391–413.

Martinez-Ruiz, F., Kastner, M., Paytan, A., Ortega-Huertas, M., Bernasconi, S.M., 2000. Geochemical evidence for enhanced productivity during S1 sapropel deposition in the eastern Mediterranean. Paleoceanography 15, 200–209.

Martinez-Ruiz, F., Paytan, A., Kastner, M., Gonzalez-Donoso, J.M., Linares, D., Bernasconi, S.M., Jimenez-Espejo, F.J., 2003. A comparative study of the geochemical and mineralogical characteristic of the sapropel S1 in the western and eastern Mediterranean. Palaeogeog. Palaeoclimatol. Palaeoecol. 190, 23–37.

Mercone, D., Thomson, J., Croudace, I.W., Siani, G., Paterne, M., Troelstra, S., 2000. Duration of S1, the most recent sapropel in the eastern Mediterranean Sea, as indicated by accelerator mass spectrometry radiocarbon and geochemical evidence. Paleoceanography 15 (3), 336–347.

Murat, A., 1991. Enregistrement sédimentaire des paléonvironments quaternaries en Méditerranée Orientale. Thése de doctorat, Université de Perpignan, 280 pp.

Murat, A., Got, H., 2000. Organic carbon variations of the eastern Mediterranean Holocene sapropel: a key for understanding formation processes. Palaeogeog. Palaeoclimatol. Palaeoecol. 158, 241–257.

Myers, P.G., Haines, K., Rohling, E.J., 2000. Modelling the paleocirculation of the Mediterranean: the last glacial maximum and the Holocene with emphasis on the formation of sapropel S1. Paleoceanography 13 (6), 586–606.

Olausson, E., 1961. Studies of deep sea cores. Reports of the Swedish Deep-Sea Expedition, 1947–1948, Vol.8, pp. 323–438.

Paillard, D., Labeyrie, L., Yiou, P., 1996. Macintosh program performs time-series analysis. Eos Trans. AGU 77 (379).

Redfield, A.C., Ketchum, B.H., Richards, F.A., 1963. The influence of organisms in the composition of sea water. In: Hill, M.N. (Ed.), The Sea. Interscience, New York, pp. 26–77.

Rohling, E.J., 1994. Review and new aspects concerning the formation of eastern Mediterranean sapropels. Mar. Geol. 122, 1–28.

Rohling, E.J., Hilgen, F.J., 1991. The eastern Mediterranean climate at time of sapropel formation: a review. Geol. Mijnb. 70, 253–264.

Rohling, E.J., Jorissen, F.J., Vergnaud-Grazzini, C., Zachariasse, W.J., 1993. Northern Levantine and Adriatic Quaternary planktic foraminifera; reconstruction of paleoenvironmental gradients. Mar. Micropaleontol. 21, 191–218.

Rossignol-Strick, M., 1983. African monsoon, an immediate response to orbital insolation. Nature 304, 46–49.

Rossignol-Strick, M., 1985. Mediterranean Quaternary sapropels, an intermediate response of the African monsoon to variation of insolation. Palaeogeog. Palaeoclimatol. Palaeoecol. 49, 237–263.

Ryan, W.B.F., 1972. Stratigraphy of Late Quaternary sediments in the Eastern Mediterranean. In: Stanley, D.J. (Ed.), The Mediterranean Sea: A natural sedimentation laboratory. Dowden, Hutchinson & Ross, Stoudsburg, PA, pp. 149–170.

Ruttenberg, K.C., 1992. Development of a sequential extraction method for different forms of phosphorus in marine sediments. Limnol. Oceanogr. 37 (7), 1460–1482.

Sarmiento, J.L., Herbert, T., Toggweiler, J.R., 1988. Mediterranean nutrient balance and episodes of anoxia. Glob. Biogeochem. Cycles 2, 427–444.

Siani, G., Paterne, M., Arnold, M., Bard, E., Métivier, B., Tisnerat, N., Bassinot, F., 2000. Radiocarbon reservoir ages in the Mediterranean Sea and Black Sea. Radiocarbon 42 (2), 271–280.

Skilbeck, C.G., Rolph, T.C., Hill, N., Woods, J., Wilkens, R.H., 2005. Holocene millennial/centennial-scale multiproxy cyclicity in temperate eastern Australian estuary sediments. J. Quat. Res. 20 (4), 327–347.

Slomp, C.P., Van der Gaast, S.J., Van Raaphorst, W., 1996. Phosphorus binding by poorly crystalline iron oxides in North Sea sediments. Mar. Chem. 52, 55–73.

Slomp, C.P., Thomson, J., De Lange, G., 2002. Enhanced regeneration of phosphorous during formation of the most recent eastern Mediterranean sapropel (S1). Geochim. Cosmochim. Acta 66 (7), 1171–1184.

Slomp, C.P., Thomson, J., De Lange, G., 2004. Controls on phosphorus regeneration and burial during formation of eastern Mediterranean sapropels. Mar. Geol. 203, 141–159.

Stratford, K., Williams, R.G., Myers, P.G., 2000. Impact of the circulation on sapropel formation in the eastern Mediterranean. Glob. Biogeochem. Cycles 14 (2), 683–695.

Stuiver, M., Grootes, P.M., Braziunas, T.F., 1995. The GISP2 $\delta^{18}O$ record of the past 16,500 years and the role of the sun, ocean and volcanoes. Quat. Res. 44, 341–354.

Tamburini, F., Huon, S., Steinmann, P., Grousset, F.E., Adatte, T., Föllmi, K.B., 2002. Dysaerobic conditions during Heinrich event 4 and 5. Evidence from phosphorus distribution in a North Atlantic deep-sea core. Geochim. Cosmochim. Acta 66 (23), 4069–4083.

Tamburini, F., Föllmi, K.B., Adatte, T., Bernasconi, S.M., Steinmann, P., 2003. Sedimentary phosphorus record from the Oman margin: new evidence of high productivity during glacial periods. Paleoceanography 18 (1), 1015.

Thomson, J., Higgs, N.C., Wilson, T.R.S., Croudace, I.W., De Lange, G.J., van Santvoort, P.J.M., 1995. Redistribution and geochemical behaviour of redox-sensitive elements around S1, the most recent eastern Mediterranean sapropel. Geochim. Cosmochim. Acta 59 (17), 3487–3501.

Thomson, J., Mercone, D., De Lange, G., van Santvoort, P.J.M., 1999. Review of recent advances in the interpretation of eastern Mediterranean sapropel S1 from geochemical evidences. Mar. Geol. 153, 77–89.

Troelstra, G., Gansenn, G.M., Van Der Borg, K., De Jong, A.F.M., 1991. A late Quaternary stratigraphic framework for eastern Mediterranean sapropel S1 based on AMS ^{14}C dates and stable oxygen isotopes. Radiocarbon 33 (1), 15–21.

Turney, C., Baillie, M., Clemens, S., Brown, D., Palmer, J., Pilcher, J., Reimer, P., Leuschner, H.H., 2005. Testing solar forcing of pervasive Holocene cycles. J. Quat. Sci. 20 (6), 511–518.

Tyson, P.D., Cooper, G.R.J., McCarthy, T.S., 2002. Millenial to multi-decadal variability of the climate of Southern Africa. Int. J. Climatol. 22, 1105–1117.

Van Santvoort, P.J.M., De Lange, G.J., Thomson, J., Cussen, H., Wilson, T.R.S., Krom, M.D., Ströhle, K., 1996. Active post-depositional oxidation of the most recent sapropel (S1) in sediments of the Eastern Mediterranean Sea. Geochim. Cosmochim. Acta 60 (21), 4007–4024.

Wehausen, R., Brumsack, H.J., 1998. The formation of eastern Mediterranean sapropels: constraints from high-resolution major and minor element studies. In: Robertson, A.H.F., Emeis, K.-C., Richter, C., Camerlenghi, A. (Eds.), Proc. ODP, Sci. Results, 160. Ocean Drilling Program, College Station, TX, pp. 207–217.